



Amorphous solid dispersions of lidocaine and lidocaine HCl produced by ball milling with well-defined RAFT-synthesised methacrylic acid polymers

Sara E. Bakhtiari^a, Zilan Zhu^a, Oxana V. Magdysyuk^b, Steve Brocchini^a, Gareth R. Williams^{a,*}

^a UCL School of Pharmacy, 29-39 Brunswick Square, WC1N 1AX London, United Kingdom

^b Diamond Light Source, Harwell Science and Innovation Campus, Didcot, Oxfordshire OX11 0DE, United Kingdom

ARTICLE INFO

Keywords:

Amorphous solid dispersion
Poly(methacrylic acid)
Lidocaine

ABSTRACT

This study focuses on the use of methacrylic acid polymers synthesised via the Reversible Addition Fragmentation chain Transfer (RAFT) polymerisation method for the production of amorphous solid dispersions (ASDs) by ball milling, to kinetically solubilize a poorly water-soluble model drug. The solid-state characteristics and the physical stability of the formulations were investigated using X-ray diffraction, differential scanning calorimetry, and infrared spectroscopy. This was followed by dissolution studies in different media. It was discovered that the acidic polymers of methacrylic acid were capable of interacting with the weakly basic drug lidocaine and its hydrochloride salt form to produce ASDs when a polymer to drug ratio of 70:30 w/w was used. The ASDs remained amorphous following storage under accelerated aging conditions (40 °C and 75% relative humidity) over 8 months. Fast dissolution and increased lidocaine solubility in different media were obtained from the ASDs owing to the reduced microenvironment pH and enhanced solubilization of the drug caused by the presence of the acidic polymer in the formulation. Production of ASDs using well-defined RAFT-synthesised acidic polymers is a promising formulation strategy to enhance the pharmaceutical properties of basic poorly water-soluble drugs.

1. Introduction

Oral drug delivery is cost-effective, non-invasive, and the most commonly used route of administration (Baghel et al., 2016). To reach the blood circulation, orally administered active pharmaceutical ingredients (APIs) must permeate across the gut intestinal membrane. They must therefore first dissolve in gastrointestinal (GI) fluid to get absorbed and distributed throughout the body. Hence, the bioavailability of many APIs and their clinical efficacy depend on their solubility and dissolution rate in the GI tract. The Biopharmaceutical Classification System (BCS) was introduced in 1996 by Amidon et al. (1995) and classifies APIs into 4 groups based on their solubility and permeability. Among the groups, BCS class II compounds have high permeability and low aqueous solubility. Many marketed drugs, as well as 50–60% of the APIs in development, belong to this class (Ku, 2008), and require significant formulation development to prepare an effective medicine.

To increase the dissolution rate of these compounds, many formulation strategies have been utilized, including particle size reduction, salt formation, and production of amorphous solid dispersions (ASDs) (Baghel et al., 2016). Drugs in their crystalline form are

thermodynamically stable and have strong intermolecular forces which provide an energy barrier to dissolution. Amorphous materials, on the other hand, lack long range order and possess no crystal lattice energy barrier to dissolution (Baghel et al., 2016). For the production of ASDs, a drug is typically mixed with a physiologically inert polymeric carrier (Craig, 2002).

Many processes have been used for the production of ASDs including hot-melt extrusion (HME), spray drying, and ball milling (Bhujbal et al., 2021). Mechanical milling of API and polymer is a simple and scalable method for preparing ASDs, and generates high yields of very fine particles by applying shear force to break the lattice of the drug and mix the components together (Fan et al., 2019). This technique is suitable for formulating thermally unstable drugs and does not require use of solvents, which has resulted in interest from industry. Ball milling in combination with HME was for instance used in the development of an oral formulation of olaparib for treatment of relapsed ovarian cancer (Hughes, 2017).

The amorphous phase and the stability of a formulation can be prolonged by choosing a suitable polymer capable of interacting with the drug, reducing its molecular mobility, and thus inhibiting

* Corresponding author.

E-mail address: g.williams@ucl.ac.uk (G.R. Williams).

<https://doi.org/10.1016/j.ijpharm.2023.123291>

Received 3 May 2023; Received in revised form 14 July 2023; Accepted 1 August 2023

Available online 5 August 2023

0378-5173/© 2023 The Author(s). Published by Elsevier B.V. This is an open access article under the CC BY license (<http://creativecommons.org/licenses/by/4.0/>).

crystallisation (Konno et al., 2008). Hydrophilic polymers are commonly used as they enhance wettability and accelerate dissolution of poorly water-soluble drugs (Bhujbal et al., 2021). Methacrylate-based polymers, such as the Eudragit E polymers (cationic copolymers made up of dimethylaminoethyl methacrylate, butyl methacrylate, and methyl methacrylate) are hydrophilic and amorphous in nature and hence suitable for ASD generation. These polymers were reported to form ASDs with itraconazole and indomethacin, respectively (Liu et al., 2010; Soti et al., 2015). Similarly, Mesallati et al. reported that acidic methacrylate-based polymers including Eudragit L100 and L100-55 interacted with the positively charged secondary amine group of ciprofloxacin and formed ASDs with enhanced solubility in water and simulated intestinal fluid (Mesallati et al., 2017). Eudragit L100-55 and L100 have also been reported to improve the dissolution properties of nintedanib by enhancing its solubility and maintaining drug supersaturation (Qin et al., 2022), and Eudragit L100-55 has previously been used to prepare ASDs with lidocaine and lidocaine hydrochloride (Liu et al., 2018). It was reported that the different forms of lidocaine resulted in different drug-polymer interactions. Acid-base ionic interactions between lidocaine and Eudragit L100-55 only occurred when lidocaine in its free base form was used in the formulation. This interaction was found to be the reason why the lidocaine-Eudragit L100-55 system was physically more stable than the lidocaine HCl-Eudragit L100-55 material during storage.

In previous work, we applied RAFT polymerisation to prepare a family of poly(methacrylic acid) (PMAA) polymers with controlled molecular weight and narrow molecular weight dispersion, and used those to prepare polyelectrolyte complexes (Bakhtiari et al., 2023). Here, we explore the ability of the PMAA polymers to form ASDs with lidocaine (2-diethylamino-N-(2,6-dimethylphenyl)acetamide) as a model drug. Lidocaine (LID) is a commonly used local anaesthetic and has antibacterial and antifungal properties (Zotova et al., 2020). It is a weak base with a pK_a of 7.9. The absorption of the drug in its free base form is limited by its dissolution rate, and therefore LID is considered to be a BCS class II drug. The ability of our new methacrylic acid polymers to interact with LID in its free base and hydrochloride salt forms and produce ASDs via ball milling was assessed, and the resultant materials characterized in detail. By dint of these studies, we sought to explore whether highly monodisperse low-molecular weight polymers could be used to stabilize LID ASDs in the same manner as the high molecular weight and polydisperse Eudragit family.

2. Materials and methods

2.1. Materials

Methacrylic acid (MAA), 4-cyano-(phenyl-carbonothioylthio) pentanoic acid (CTA), azobisisobutyronitrile (AIBN), polyvinylpyrrolidone (PVP, Mw = 10000 Da), poly(acrylic acid) (PAA, Mw = 1800 Da), lidocaine, and lidocaine hydrochloride were purchased from Sigma-Aldrich. Methanol (MeOH, 100%) was purchased from VWR Chemicals. Deuterated dimethyl sulfoxide (d_6 -DMSO) was supplied by Cambridge Isotope Laboratories. Fasted state simulated intestinal fluid (FaSSIF) pH 6.5 was purchased from Fisher Scientific.

2.2. Methods

2.2.1. Synthesis of PMAA

The synthesis of methacrylic acid polymers via RAFT polymerisation was carried out as previously reported (Bakhtiari et al., 2023). Briefly, for synthesis of PMAA with degree of polymerisation (the number of repeat units in an average polymer chain) of 80, methacrylic acid (1 g, 11.61 mmol, 80 eq.), CTA (41 mg, 0.14 mmol, 1 eq.) and AIBN (2.38 mg, 0.014 mmol, 0.1 eq.) were dissolved in methanol (7 ml) in a 25 ml single neck round bottomed flask. The reaction mixture was sealed with a rubber septum and purged using argon for 30 min; the flask was then

heated at 70 °C for 17 h under magnetic stirring. The reaction was stopped by exposing the solution to air via a needle and the polymer was precipitated twice in 70 ml of cooled diethyl ether ($10 \times$ the volume of methanol) with mild stirring. The obtained polymer was then washed with methanol (6 ml) and dried using rotatory evaporation and vacuum. The same procedure was repeated for synthesis of methacrylic acid polymers with degree of polymerisation of 20.

2.2.2. Ball milling

Lidocaine was milled with each polymer (PAA, PVP, and PMAA with DP of 20 and 80 [PMMA₂₀ and PMMA₈₀]) at a concentration of 30, 50, and 70% (w/w). Lidocaine HCl was milled with PMAA₈₀ and PVP. Milling was performed at room temperature using a Form-Tech Scientific FTS1000 mill. 1 g of solid material was added to 20 ml stainless steel grinding jars. Two stainless steel milling balls with 7 mm diameters were used. Samples were milled for one hour at a frequency of 30 Hz (1800 rpm).

2.2.3. X-ray diffraction (XRD)

XRD was performed using a MiniFlex 600 diffractometer (Rigaku) supplied with Cu K α radiation (1.5418 Å). Samples were scanned from 3 to 50° 2 θ in steps of 0.02°. The scan rate was 5°/min. The output voltage and current were 40 kV and 15 mA, respectively.

2.2.4. Thermogravimetric analysis (TGA)

TGA was carried out using a Discovery instrument (TA Instruments, Waters LLC). Nitrogen was used as the purge gas with a flow rate of 25 ml/min. 5–8 mg samples were analysed in aluminium pans. Samples were heated from 40 to 300 °C at a rate of 10 °C/min.

2.2.5. Differential scanning calorimetry (DSC)

DSC was carried out using a Q2000 instrument (TA Instruments, Waters LLC). Nitrogen was used as the purge gas. 3–7 mg of each sample was analysed in TA Instruments Tzero aluminium pans sealed with non-hermetic lids. Polymer samples and ASDs were heated from –80 to 100 °C at a rate of 10 °C/min. The theoretical glass transition (T_g) values of the ASDs were calculated using the Gordon-Taylor equation (1).

$$T_g = (w_1 T_{g1} + k w_2 T_{g2}) / (w_1 + k w_2) \quad (1)$$

where w_1 and w_2 refer to the weight fractions of the ASD components, T_g is the glass transition temperature of the mixture, T_{g1} and T_{g2} correspond to the glass transition temperatures of each component, and k is the difference in the heat capacity of the components when they transition from the glass form to the rubbery state. This can be calculated from equation (2), where ρ_1 and ρ_2 refer to the densities of the components.

$$K = T_{g1} \rho_1 / T_{g2} \rho_2 \quad (2)$$

2.2.6. Differential scanning calorimetry – X-ray diffraction (DSC-XRD)

Simultaneous DSC-XRD experiments were performed on Beamline I12 at the Diamond Light Source (Clout et al., 2016; Drakopoulos et al., 2015). A modified TA Instruments Q20 DSC and a monochromatic X-ray beam (size 0.5 mm \times 0.5 mm, $\lambda = 0.2441$ Å) aligned with the holes on the furnace were used. Diffraction data were collected using a Pilatus 2 M CdTe detector (Šišak Jung et al., 2017). X-ray energy and sample-detector distance were calibrated with CeO₂ using DAWN Science Workbench (Basham et al., 2015; Filik et al., 2017; Hart et al., 2013). Samples (9–13 mg) were loaded into sealed Tzero aluminium pans (TA Instruments, USA) and heated at a rate of 10 °C/min from 40 to 75 °C. Samples were then cooled down to 40 °C followed by a second heating cycle at 10 °C min⁻¹ from 40 °C to 75 °C. Diffraction patterns were recorded every 6 s. The DAWN Science Workbench was used to perform azimuthal integration, normalize for the beam current, and subtract the background. Data were plotted using the OriginPro 2021 software.

2.2.7. Fourier transform infrared spectroscopy (FTIR)

A Perkin-Elmer Spectrum 100 attenuated total reflection-FTIR spectrometer was employed to collect spectra over the range of 650–4000 cm^{-1} , at a resolution of 4 cm^{-1} , with 8 scans obtained.

2.2.8. Stability study

Stability studies were carried out under accelerated storage conditions of 40 °C and 75% relative humidity (RH). Samples were analysed by XRD and DSC every week in the first month and then once every 4 weeks. Dynamic vapor sorption (DVS) was used to further investigate stability at elevated RH, using a Q5000 SA instrument (TA Instruments, Waters LLC). 10–15 mg of fresh sample was used for each run. The temperature was maintained at 25 °C, while the RH was equilibrated at 0% until the percentage weight change was lower than 0.01% for 5 min. RH was then raised to 90% at a rate of 0.5% min^{-1} , before being reduced to 0% at 0.5% min^{-1} .

2.2.9. Dissolution studies

An excess amount of the drug with respect to the expected water solubility of lidocaine (5x the thermodynamic solubility) in its pure form or as an ASD (80–270 mg) was added to a vial filled with 8 ml of 0.1 M phosphate buffered saline (PBS) with pH of 7.4. The vials were placed in an incubator at 37 °C under stirring. At various time points over 2 h, 0.5 ml aliquots were taken from each sample and filtered with 0.45 μm filters. The filtered samples were then diluted and the concentration of the drug in each sample was determined on an Agilent Cary 60 UV–Vis spectrophotometer at 226 nm. Dissolution of lidocaine and lidocaine HCl was also explored in two acidic media; fasted state simulated intestinal fluid (FaSSIF, pH 6.5) and fasted state simulated gastric fluid (FaSSGF, pH 2). FaSSGF was generated by adding HCl to FaSSIF to reduce the pH to 2. The pH of each sample was recorded before and after

the 2 h timepoint using a HI 2210 pH meter (Hanna Instruments). Additional experiments in PBS were performed under sink conditions. These were undertaken by adding an equivalent of 0.4 mg/ml of lidocaine in the form of the pure drug or ASD (3.2–9.6 mg) to 8 ml of solvent. Dissolution of ASD samples stored for 8 weeks under accelerated aging conditions was further investigated to compare the dissolution profiles of freshly prepared and aged samples.

3. Results

3.1. Formation of amorphous solid dispersions

MAA polymers with DP of 80 (7200 Da) and 20 (2000 Da) were synthesised using RAFT polymerization following the same protocols as used in our previous work (Bakhtiari et al., 2023). The NMR spectra, chemical structure and the GPC traces of the polymers can be found in the Supplementary Information, Figure S1 and S2.

Ball milling has been reported to be a suitable method to form ASDs of poorly water-soluble drugs (Mesallati et al., 2017). Three different ratios of PMAA₈₀ to LID (30%, 50%, and 70% w/w PMAA₈₀) were milled for 1 h at room temperature. Before milling, XRD analysis showed a decrease in the intensity of the LID Bragg reflections as the ratio of the polymer to drug increased, owing to dilution. After milling, the XRD of the sample with the highest weight ratio of the polymer (70% w/w PMAA₈₀) displayed only broad haloes characteristic of amorphous material (Fig. 1a). The absence of the LID melting endotherm at 68.5 °C and presence of a T_g (at -13.9 °C) in the DSC thermogram of this sample confirmed its amorphous nature (Fig. 1b). The theoretical T_g calculated using the Gordon-Taylor equation was -26.4 °C. A positive deviation (experimental T_g > theoretical T_g) was recorded for this formulation, which suggests the existence of strong interactions between the polymer

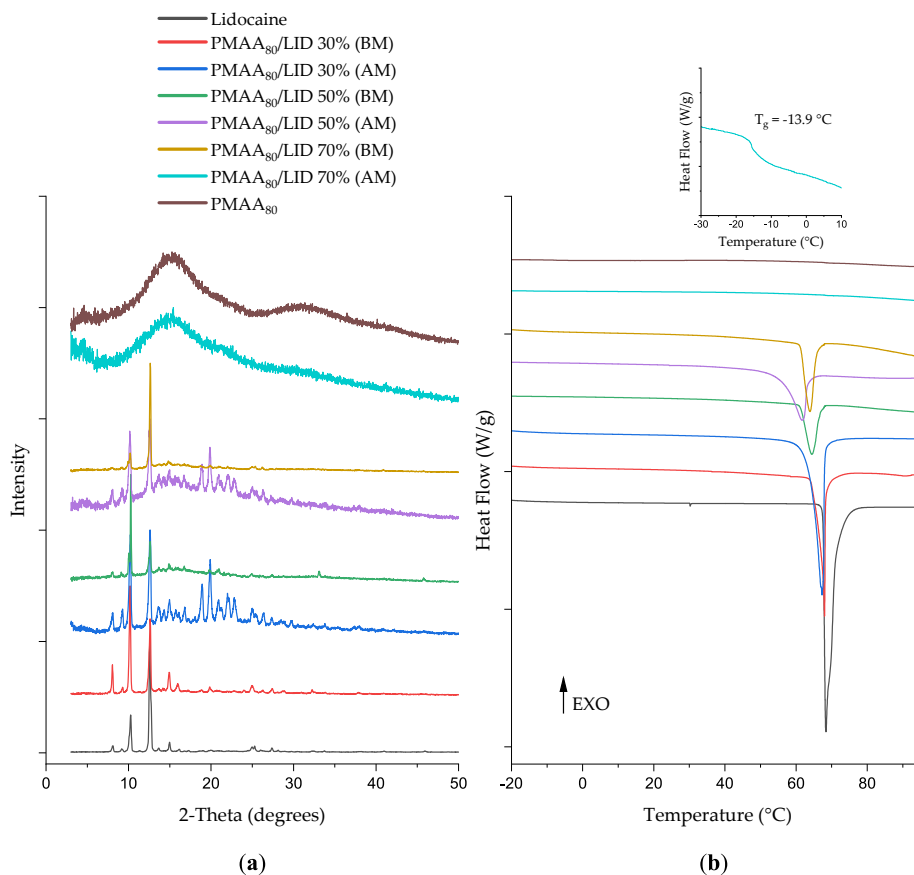


Fig. 1. (a) XRD analysis and (b) DSC thermograms of LID, PMAA₈₀, and mixtures with 30, 50, and 70% w/w PMAA₈₀ before (BM) and after milling for 1 h (AM).

and the drug. After milling, XRD and DSC analysis of the formulations with 30% and 50% PMAA₈₀ still showed characteristic lidocaine Bragg reflections and melting endotherms respectively, demonstrating the presence of crystalline material. These formulations hence did not produce fully amorphous material, presumably owing to the relatively low amount of polymer present.

The PMMA₈₀-LID 70/30 % w/w ASD was further analysed using DSC-XRD. Initially, the dispersion of PMMA and lidocaine before milling (Fig. 2a) can be seen to be crystalline. However, as the temperature in the system increased, and following the LID melting point at 65 °C, the Bragg reflections disappeared. The system remains amorphous during cooling, and no recrystallisation is observed during a second heating cycle. The ball milled PMMA/lidocaine is amorphous, with no Bragg reflections visible at any point during the heat/cool/heat cycles (Fig. 2b). The corresponding DSC thermograms can be found in Figure S3 and Figure S4.

To examine whether the degree of polymerisation of poly(methacrylic acid) impacts the formation of LID ASDs, PMAA with a DP of 20 (PMMA₂₀) was milled with lidocaine. The XRD and DSC results revealed that the formulation with 70% w/w PMAA₂₀ and 30% lidocaine was amorphous in nature following ball milling for 1 h, while the systems with reduced polymer content again displayed crystalline features (Figure S5). For comparison, LID was also milled with PVP and PAA (amorphous polymers that have previously been used to generate ASDs of poorly water-soluble drugs (Turner and Schwartz, 2022; Xie and Taylor, 2016)). Unlike the situation with PMAA, this did not lead to the production of ASDs at any w/w ratio of LID-polymer explored (Figure S6 and S7).

To assess the effect of drug form on the formation of ASDs using MAA polymers, PMAA₈₀ was milled with lidocaine hydrochloride. Similar to the PMAA₈₀/LID samples, milled samples of PMAA₈₀/LID HCl with 70% w/w polymer in the formulation were amorphous in nature, while those using lower polymer concentrations retained crystalline character. After milling, the XRD pattern of the 70/30% w/w sample contained only broad haloes and the DSC thermogram showed no sign of a melting endotherm (Fig. 3). The milled samples of PMAA₈₀/LID HCl displayed a T_g at 12.41 °C, greater than the theoretical T_g (5.3 °C), which suggests strong interactions within the polymer-drug complex. Lidocaine HCl was also milled with PVP. The presence of a small melting endotherm in

the DSC thermogram and Bragg reflections in the XRD patterns of the milled samples, even at 70% w/w polymer, indicate that the samples were not fully amorphous (see Figure S8).

3.2. Solid state characterisation of the ASDs

The thermal degradation of the pure drug and the milled samples was tested using TGA and their mass loss profiles are shown in Figure S9. The ASDs lost 3–5% of their mass below 150 °C through water evaporation. Initial water loss at around 100 °C is commonly observed in the TGA of ASDs with hydrophilic polymers, and these findings are hence in accord with the literature (Mesallati et al., 2017).

The interactions between PMAA₈₀ and the drugs were analysed using FTIR. The bands at 3250 cm⁻¹ and 2800 cm⁻¹ in the FTIR spectrum of LID free base in Fig. 4 were assigned to the N–H stretching of the amide group and C–H stretching, respectively. The lidocaine tertiary amine produced signals in the 1000–1360 cm⁻¹ region. The vibrations at 1661 cm⁻¹ and 1488 cm⁻¹ were assigned to C = O stretching of the amide group and the secondary amide N–H bending, respectively. In the FTIR spectrum of the polymer, the band at 1700 cm⁻¹ can be attributed to C = O stretching of the carboxylic acid group.

The 70% w/w polymer/drug formulation after milling displayed a similar spectrum to that of the pure polymer. There is only one clear signal in the 1612–1761 cm⁻¹ region, attributed to C = O stretching. The milled sample produced broader peaks compared to those visible before milling. In the spectra of the sample before milling, the bands attributing to lidocaine (e.g., at 3250 cm⁻¹ and 1661 cm⁻¹) exist with lower intensity than in the pure drug. These peaks are not visible in the spectrum of the milled ASD. The main difference between these samples is the presence of a distinct peak at 1544 cm⁻¹ in the FTIR spectrum of the milled ASD. This peak is attributed to the drug molecule's tertiary amine R₃N⁺-H group, which indicates that after milling the drug exists in its ionised form in the polymer matrix (see Fig. 5) (Liu et al., 2018). This means that acid-base interactions between the drug and the polymer must have been generated during ball milling. This peak can only be seen when a polymer: drug ratio of 70: 30 w/w is used, which indicates that an excess amount of methacrylic acid was needed to produce the interaction with the drug. The FTIR spectra of the three milled formulations at different weight ratios are shown in Figure S10. The spectra of

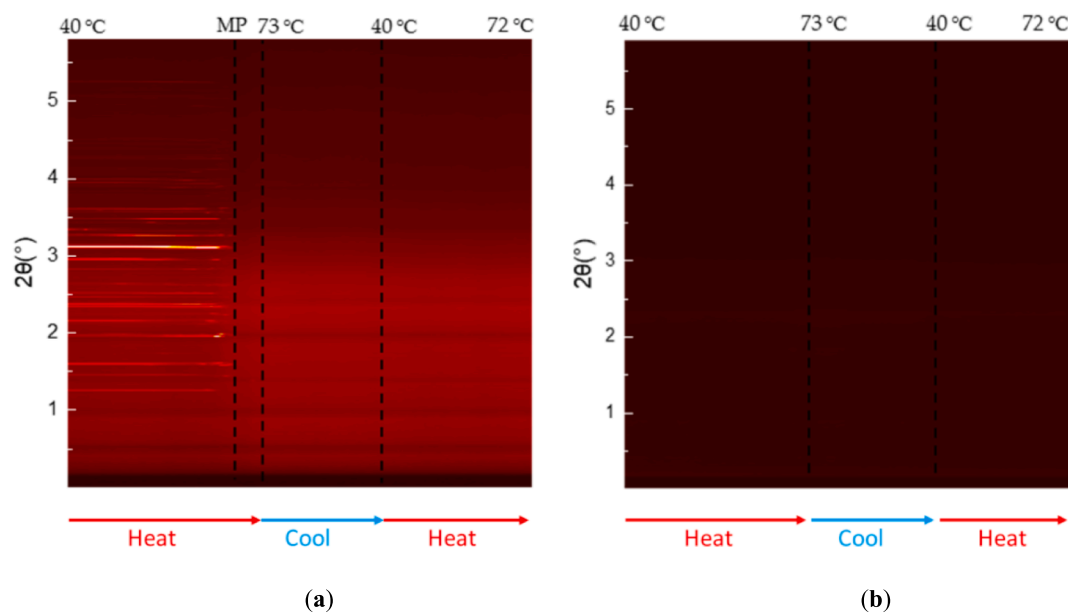


Fig. 2. Contour XRD-DSC plots of PMAA/LID (a) before and (b) after milling. Brighter colours correspond to more intense Bragg reflections, while dark colours indicate a lack of crystalline material. These experiments were performed using X-rays of wavelength 0.2441 Å, which results in the reflections appearing at lower angle than in a standard lab XRD pattern.

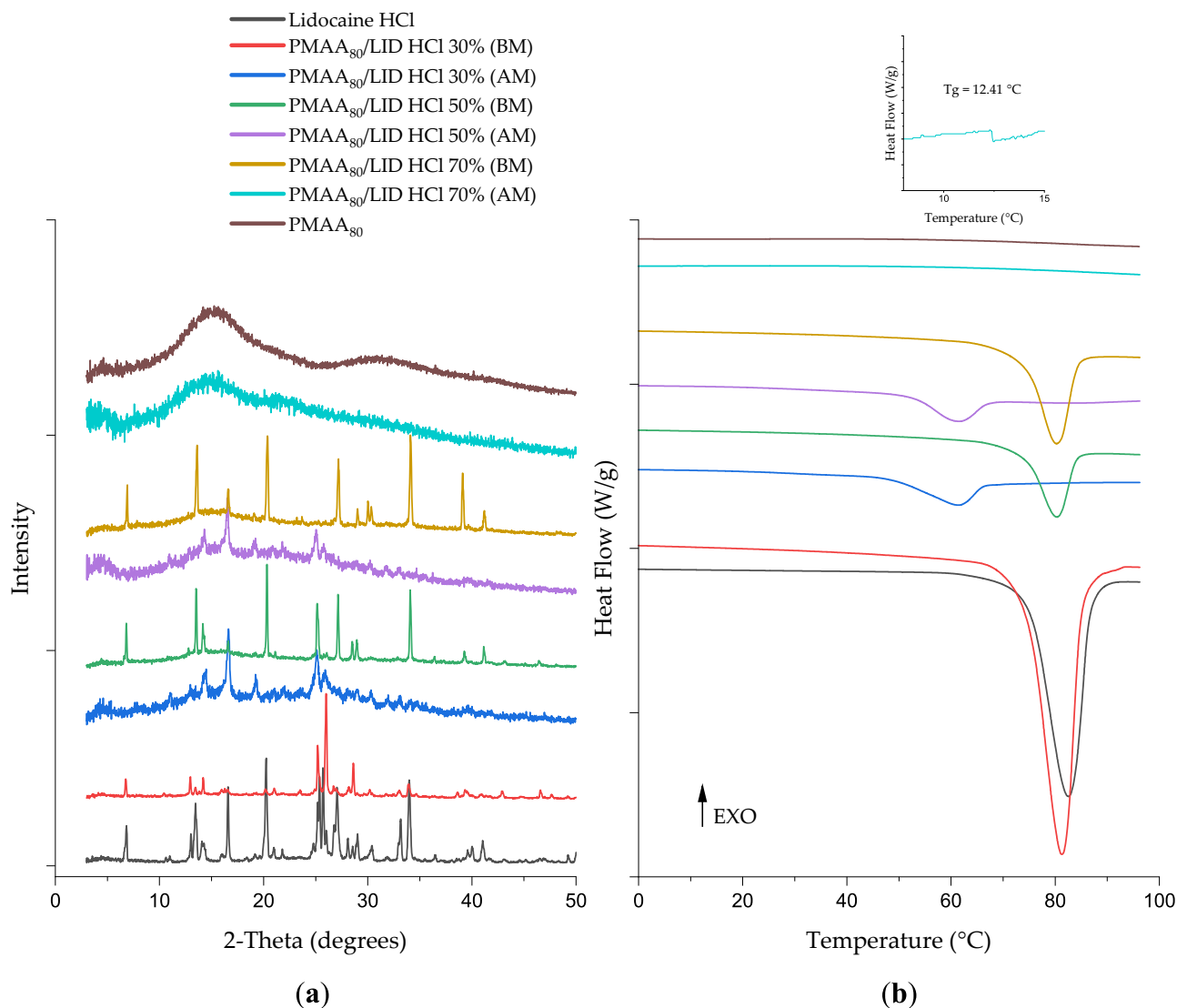


Fig. 3. (a) XRD and (b) DSC data of 30, 50, and 70% w/w PMAA₈₀/LID HCl mixtures before (BM) and after milling for 1 h (AM).

the 30% and 50% w/w PMAA₈₀/LID samples show sharp peaks resembling the spectrum of the crystalline drug. The C = O band of the polymer appears as a small shoulder on the left (higher wavenumber) of the signal corresponding to the C = O stretching of lidocaine's amide group.

Fig. 6 shows the FTIR spectrum of LID HCl. N–H stretching can be seen at 3390 and 3450 cm⁻¹ and the C = O stretching band is at 1655 cm⁻¹. The two sharp peaks at 1473 cm⁻¹ and 1543 cm⁻¹ were assigned to the N–H bending of the drug molecule's secondary amide and the tertiary amine N⁺-H. This peak could also be observed in the spectra of all three of the PMAA₈₀/LID HCl formulations, as seen in Figure S11. However, according to the XRD and DSC results, only the formulation with 30% w/w LID HCl gave sufficient intermolecular interactions to form an ASD. Similar FTIR results of LID and LID HCl were reported by Liu et al. where the interaction between Eudragit L100-55 and LID in its free base and hydrochloride salt form were investigated (Liu et al., 2018).

Unlike the physical mixture sample (before milling), the spectrum of the milled sample in Fig. 6 displays a broad band in the 1580–1766 cm⁻¹ region. The bands at 3390 cm⁻¹ and 3450 cm⁻¹ are not visible for the milled sample, which indicates the existence of strong polymer/drug interactions and that the drug is well dispersed in the polymer. The differences in the FTIR spectrum of the samples before milling and the

milled samples indicate that interactions between the amine group of the drug and the carboxylic acid group of PMAA₈₀ are generated during the ball milling process.

3.3. Stability studies

High temperatures and high humidity could result in an increase in molecular mobility in ASDs and cause phase separation and recrystallisation of the drug (Lin et al., 2018). This is perhaps a particular concern in this work, given the low T_g values of the ASDs generated. To investigate the stability of PMAA₈₀/LID and PMAA₈₀/LID HCl ASDs and their ability to maintain their amorphous form over time in environments with high humidity and high temperature, samples were stored under accelerated aging conditions (40 °C and 75% RH). The XRD and DSC data for the aged samples were found to be the same as those of the freshly milled samples. According to the XRD patterns shown in Fig. 7a, the samples remained amorphous after 8 months of storage in both conditions, and the DSC thermograms of the aged samples similarly showed no visible melting endotherm (Fig. 7b).

A drug in its amorphous form has higher free energy compared to its crystalline form which means that recrystallisation is thermodynamically favoured (Bhujbal et al., 2021). The energy of the amorphous material during storage can also be reduced to a more stable/lower

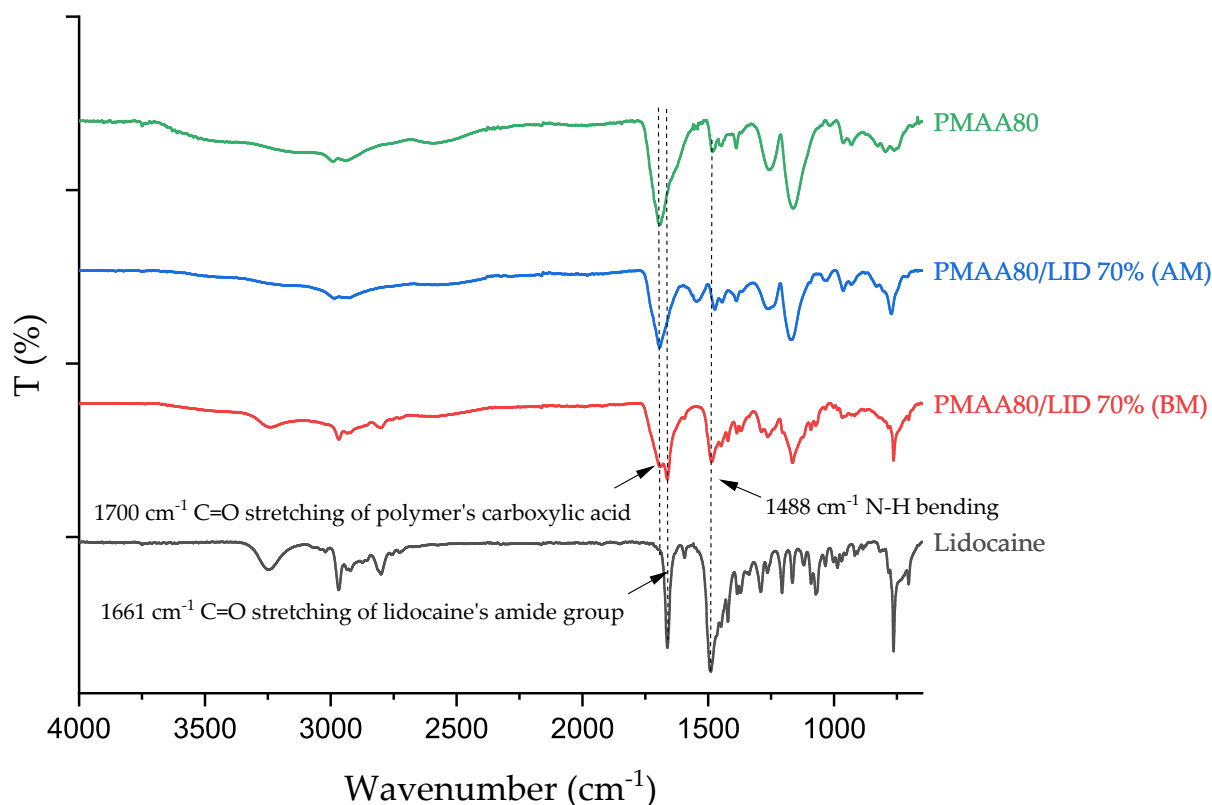


Fig. 4. FTIR spectra of PMAA₈₀, LID, and 70% w/w PMAA₈₀/LID before (BM) and after (AM) ball milling.

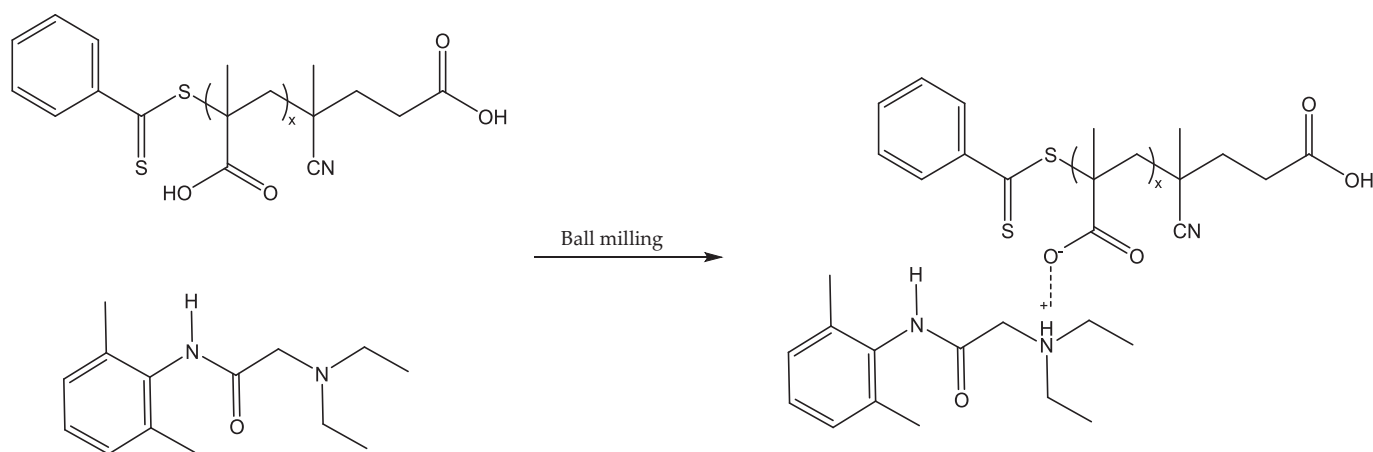


Fig. 5. An illustration of the interaction between the carboxylate group of PMAA and the ionised tertiary amine group of LID following ball milling.

energy state without recrystallisation (Graeser et al., 2010). This is called relaxation. Either process could occur over time and cause a reduction in the excess energy present in the ASD, thus resulting in a decline in the dissolution rate and solubility of the drug. However, in this study, the stability of the aged ASD samples was found to be unaffected by storage. There was no sign of relaxation (usually appearing as an endothermic event near the glass transition) in the DSC thermograms of the ASDs, nor of melting endotherms (or Bragg reflections in XRD). This suggests that the low T_g of the samples did not cause acceleration of the molecular mobility and did not impact their physical stability.

According to DVS results (Figure S12), LID gains very little mass (0.5%) after raising the relative humidity from 0 to 90%. Under the same conditions, PMMA₈₀ and the PMMA₈₀/LID 70/30% w/w physical mixture (before milling) increased in mass by 6.9% and 6.7% owing to

adsorption and absorption of water. The 70/30% w/w ASD after milling showed greater hygroscopicity, with the mass increasing by 11%. In all cases, the mass gained is lost when the humidity is reduced. Additionally, there is no sudden mass loss noted with the ASD at elevated relative humidity, indicating that the system remained amorphous and crystallisation did not occur. These findings further support the stability of the ASDs even under high-humidity conditions.

3.4. Dissolution studies

In vitro dissolution of the ASDs in PBS pH 7.4 under non-sink and sink conditions (relative to the solubility of the crystalline drug) was explored to assess their ability to generate and maintain supersaturation of the drug. Dissolution profiles of LID and the 70% w/w PMAA₈₀/LID

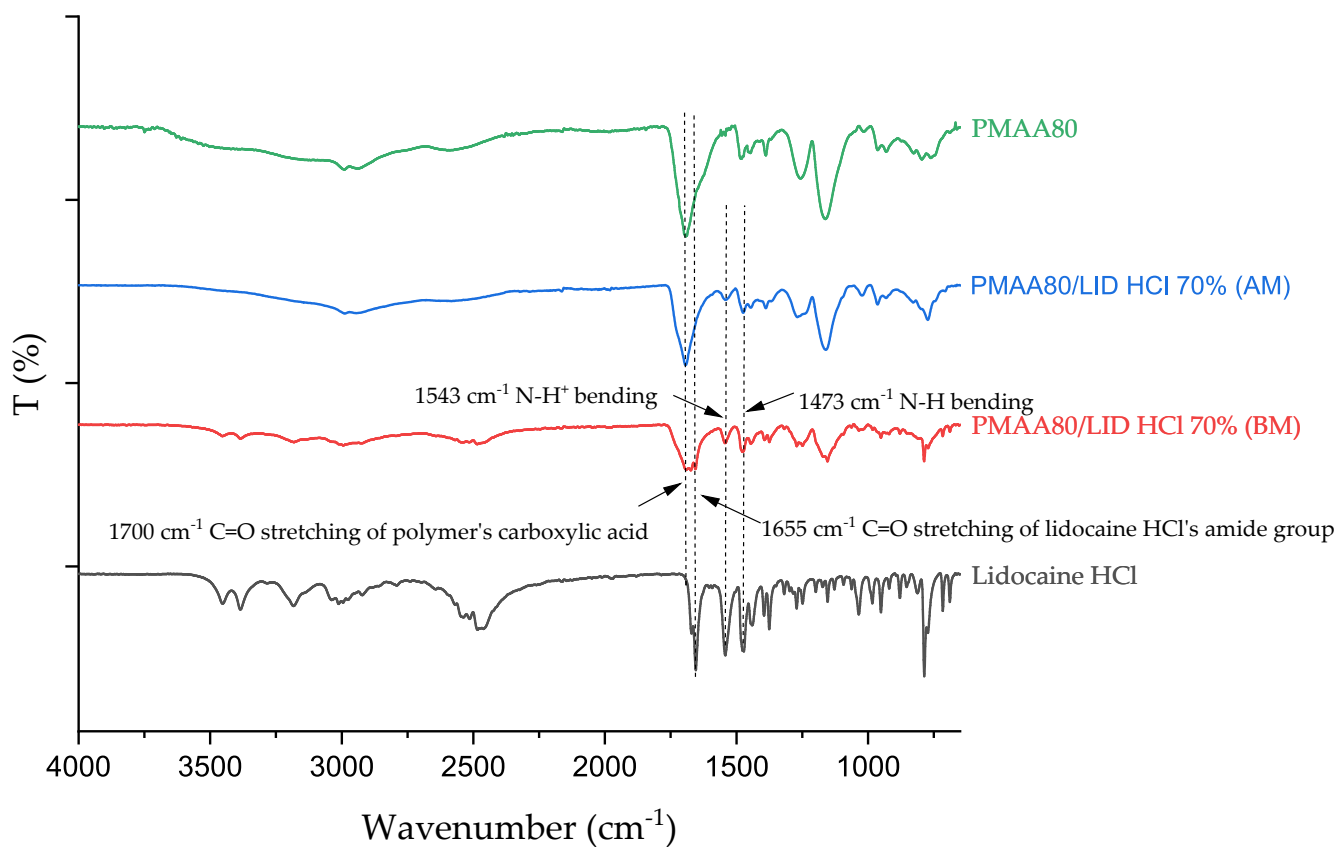


Fig. 6. FTIR spectra of PMAA₈₀, LID HCl, and 70% w/w PMAA₈₀/LID HCl mixtures before (BM) and after (AM) ball milling.

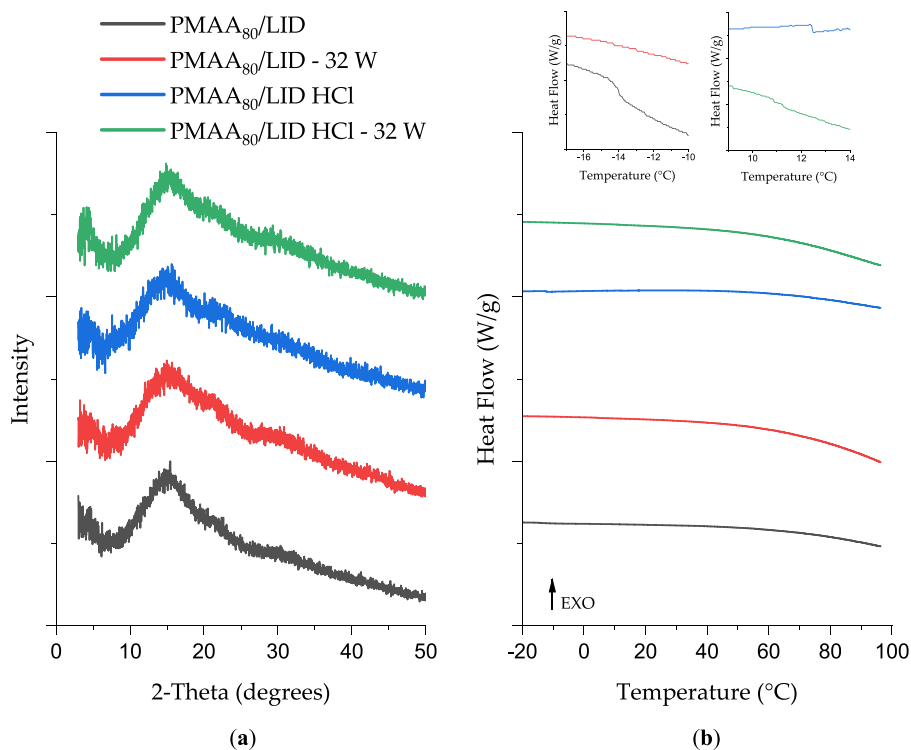


Fig. 7. (a) XRD patterns and (b) DSC thermograms of the milled 70/30 % w/w PMAA₈₀/LID and PMAA₈₀/LID HCl amorphous solid dispersions on day 0 and after 32 weeks of storage in accelerated storage conditions (40 °C, 75% RH).

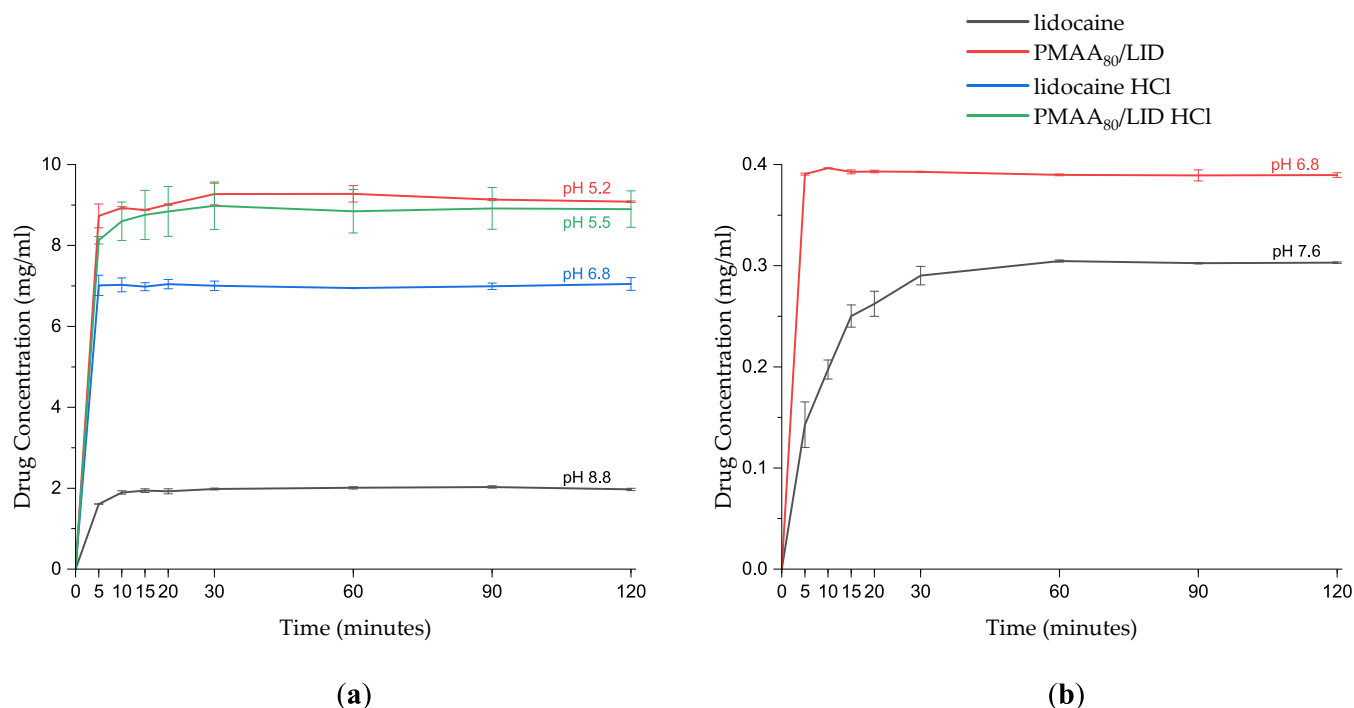


Fig. 8. Dissolution studies of LID, LID HCl and milled 70% w/w PMAA₈₀/LID and PMAA₈₀/LID HCl in PBS (pH 7.4) at 37 °C under (a) non-sink conditions and (b) sink conditions. At the end of the experiment under sink conditions, $97.4 \pm 0.2\%$ and $75.7 \pm 0.1\%$ of the drug from the ASD and pure drug samples was released into the solution, respectively. The mean pH of the solutions at the end of the experiments was recorded and is noted against the dissolution lines. The error bars represent the standard deviation ($n = 3$).

ASDs in PBS (pH 7.4) under non-sink conditions are presented in Fig. 8a. Addition of LID increased the pH of the media to 8.8. The concentration of lidocaine reached around 2 mg/ml after 15 min and remained constant. Using the Henderson-Hasselbalch equation, at pH 8.8, the solubility of lidocaine in its free base form was calculated to be 2.9 mg/ml. Under non-sink conditions, the ASD samples on average reached a concentration of lidocaine 5.4 times more than that reached by the crystalline drug. The higher solubility of the ASDs in PBS could be due to the presence of acidic MAA polymers which decreased the pH of the media to 5.2. Bergstrom et al. previously reported that the addition of acid results in an increase in the solubility of lidocaine (Bergström et al., 2004). Similarly, in our study, LID shows pH-dependent solubility. The dissolution profile of a physical mixture of the PMAA₈₀ and LID (before milling) in PBS under non-sink conditions was also investigated. Here, the concentration of LID reached a peak concentration of 7.8 mg/ml after 20 min, notably higher than the maximum concentration of the pure drug in the same conditions (Figure S13). This confirms that the solubility of lidocaine depends on pH, and the presence of the polymer caused a decrease in the pH of the solution (to pH 5.0). However, the maximum drug concentration from the physical mixture was lower than seen with the milled samples. Further, there is evidence for a spring-and-parachute effect with the sample before milling, suggesting some precipitation of LID. This is not seen with the post-milling ASD. Thus, the amorphous nature of the ASDs both increases solubility and also helps to maintain supersaturation, presumably because of the more intimate interactions between the drug and polymer in the ASD (cf. the physical mixture).

LID in its hydrochloride form is more soluble in PBS at pH 7.4 than the free base form. This is because the HCl salt dissolves and reduces the pH and increases the solubility of the drug. LID free base, on the other hand, induces an increase in the pH of the media which causes a decrease in drug solubility. The concentration of LID HCl in PBS reached a concentration of 7 mg/ml after 5 min and plateaued, while the concentration of the drug from the ASDs after 5 min was 8.1 mg/ml and increased to 9 mg/ml at the 30-min timepoint (Fig. 8a).

The dissolution profiles of lidocaine free base and PMAA₈₀/LID in PBS under sink conditions were next investigated. At the 5-min time-point, the ASDs achieved a maximum lidocaine concentration of 0.4 mg/ml in PBS, whereas the concentration of crystalline lidocaine in PBS was 0.14 mg/ml (Fig. 8b). The concentration of lidocaine from the latter sample reached 0.3 mg/ml after one hour and plateaued. The difference in dissolution rate of lidocaine in PBS under sink conditions cannot solely be attributed to changes in pH caused by addition of the polymer. The amorphous physical form of the drug as well as the presence of PMAA₈₀ in the formulation prompted the rapid dissolution of the drug. Due to their disordered structure, amorphous solid dispersions can enable more rapid dissolution of a drug to form supersaturated solutions. Hydrophilic polymers, such as the PMAA used in this study, can solubilise a drug and help maintain the supersaturated state for an extended time sufficient for the drug to get absorbed (Warren et al., 2010).

One study in the literature found that the solubility of ASDs of ciprofloxacin and Eudragit L100 in FaSSGF was lower than that of the pure crystalline drug, as the polymers used were not soluble in acidic solutions and hindered the solubilisation of the drug (Mesallati et al., 2017). To evaluate the dissolution behaviour of the ASDs in different parts of the GI tract the dissolution of LID, LID HCl, and the 70/30 % w/w PMAA₈₀/LID and PMAA₈₀/LID HCl ASDs were tested in FaSSIF and FaSSGF. The experiments were carried out under non-sink conditions with starting FaSSIF and FaSSGF pH values of 6.5 and 2, respectively. As expected, the pure LID dissolved rapidly, reaching a concentration of 8.1 mg/ml in FaSSIF (Fig. 9a). The ASD samples in FaSSIF showed similar dissolution patterns to those of the pure drugs. In FaSSGF the concentration of LID free base reached 9.9 mg/ml after 5 min (Fig. 9b). The increased solubility of basic drugs in this medium is due to the acidity of the system and presence of surfactants. The ASDs also reached a maximum drug concentration of 10 mg/ml after 5 min. The pH of FaSSGF media containing LID and ASDs measured at the end of the experiment differed only by 0.3.

The ASD samples containing LID HCl showed higher drug

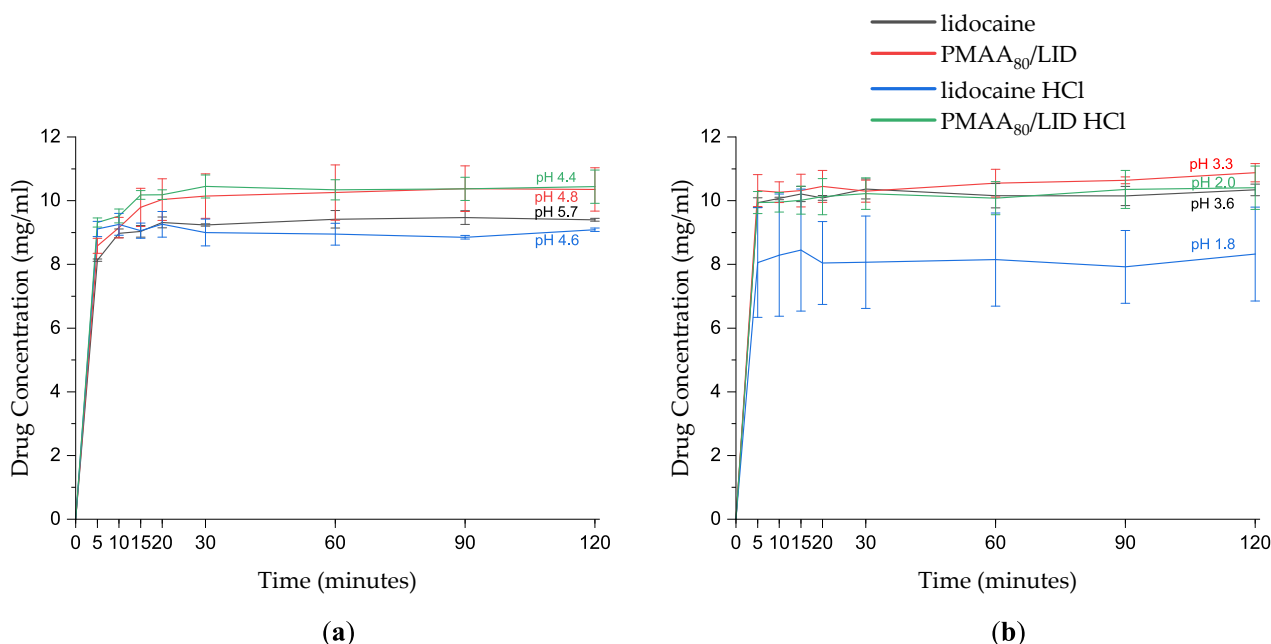


Fig. 9. Dissolution studies of LID, LID HCl and milled 70% w/w PMAA₈₀/LID and PMAA₈₀/LID HCl in (a) fasted state simulated intestinal fluid (FaSSIF), and (b) fasted state simulated gastric fluid (FaSSGF) under non-sink conditions at 37 °C. The average pH of the solutions at the end of the experiments was recorded and is noted at the right of each curve. The error bars represent the standard deviations (n = 3).

concentrations in FaSSGF compared to the pure drug. The pH of the samples containing LID HCl and the ASDs measured at the end of the experiments differed only by 0.2 units. The decreased solubility of lidocaine HCl in this media is due to the common ion effect and presence of excess counterions, which results in a decrease in the solubility of salt forms of basic drugs (Serajuddin, 2007). Elevated chloride ion concentration has also been found to decrease the dissolution rate of three different salt forms of the basic drug haloperidol (Li et al., 2005). The use of polymers in the formulations and their amorphous physical form is the reason underlying the higher solubility of lidocaine HCl in the FaSSIF and FaSSGF media compared to the pure crystalline drug.

A dissolution study of the ASDs was carried out after 8 weeks of storing the samples under accelerated aging conditions. As depicted in Figure S14, the dissolution rate and the maximum drug concentration reached in the media (water) remained unchanged. These results indicate a strong similarity between the dissolution profiles of the aged and fresh ASD samples.

4. Discussion

Preparing amorphous solid dispersions of poorly water-soluble drugs is a formulation strategy used to enhance their solubility and dissolution rate. It is well known that using polymers with high T_g in a formulation increases the T_g of the ASDs. This is termed the antiplasticisation effect. However, antiplasticisation is not the only factor responsible for reducing mobility and preventing crystallisation. The interactions between drug molecules and polymer molecules play a major role in stabilising ASD formulations and reducing the molecular mobility of the drug, thus acting to increase the energy needed for recrystallisation. Khougaz et al. reported formation of ASDs of a model drug, MK-0591 and PVP, with a lower final T_g than the T_g of the drug (Khougaz and Clas, 2000). The key factor for stabilising the formulation was found to be the existence of ion-dipole interactions between the drug's carboxylate group and PVP carbonyl group. Similarly, in this study, the presence of an R_3N^+-H bending peak and the merging of the C=O stretching bands of the drug and the polymer in the FTIR spectra of the milled samples of 70% w/w PMAA₈₀/LID and PMAA₈₀/LID HCl revealed that interactions between the amine group of the drugs and the carboxylic

acid group of the polymer were generated during the ball milling process. This interaction is the main reason the PMAA was able to inhibit crystallisation over 8 months of storage in an environment with high temperature and humidity, despite the formulations having a low T_g value.

Eudragit polymers are polymethacrylates. They have been extensively studied and are commonly used for the formation of ASDs. In a similar study, Eudragit L100-55 was used to form complexes with lidocaine and lidocaine HCl by melt extrusion (Liu et al., 2018). Both formulations consisted of 70% w/w polymer and were amorphous in nature. A positive deviation in T_g for the LID/Eudragit L100-55 formulation and a negative deviation for LID HCl/Eudragit L100-55 were reported. Following 4 months of storage at 40 °C and 70% RH, the LID HCl/Eudragit L100-55 sample crystallised, which revealed that the acid-base interaction between the polymer and LID free base was stronger than that with the polymer and the salt form of the drug. This was hypothesised to be due to protonation of the tertiary amine group of lidocaine HCl with HCl, thus hindering the interaction between the carboxylic acid groups in Eudragit L100-55 and the drug's tertiary amine. In this work, however, even though a smaller positive deviation in T_g values was observed for PMAA₈₀/LID HCl, both ASDs maintained their amorphous physical form over time.

The ASDs generated here showed pH-dependent solubility. Addition of LID to a dissolution medium was found to increase the pH, while addition of LID HCl decreased the pH. The presence of PMAA in the formulations reduced the pH of the microenvironment, which – in addition to the removal of the lattice energy barrier – resulted in an increase in the solubility of the drug. Using the PMAA₈₀/LID ASDs, a greater concentration of lidocaine in different media was achieved than with crystalline LID. In FaSSGF, LID HCl showed a slower dissolution rate and lower final drug concentration than the ASDs, which is due to the common ion effect. The drug release profiles of the PMAA₈₀/LID and PMAA₈₀/LID HCl ASDs were similar and reached a maximum concentration after 5 min. This is in contrast to the results reported by Liu et al., where at an acidic pH the drug release from the LID-Eudragit L100-55 ASD was significantly reduced (Liu et al., 2018).

5. Conclusions

This work has shown that RAFT-synthesised poly(methacrylic acid) (PMAA) was able to produce lidocaine ASDs by ball milling, via the formation of stabilising ionic interactions with the basic drug. The broad halo visible in the XRD pattern of a formulation containing 70% w/w PMAA and 30% w/w lidocaine after milling, and the absence of a melting endotherm as well as the presence of a single T_g in DSC, confirmed the amorphous physical form of the formulation. The positive deviation in the T_g of the formulation and the appearance of an N⁺-H bending peak in the FTIR spectrum of the milled samples revealed the presence of interactions between the polymer and the drug. The RAFT-synthesised polymers were also able to produce stable ASDs with the salt form of lidocaine. 70/30 % w/w PMAA/lidocaine and PMAA/lidocaine HCl formulations remained fully amorphous under accelerated aging conditions (40 °C and 75% RH) for 8 months. The ASDs also increased the dissolution rate and the maximum drug concentration reached in solution. This was achieved due to the presence of the hydrophilic polymer and the amorphous nature of the formulations as well as the reduced pH of the microenvironment caused by the dissolution of the polymer. The PMMA ASD formulations prepared in this work hence show potential for improving the physical stability and solubility of poorly water-soluble drugs.

Author Contributions

Conceptualization, G.R.W.; methodology, G.R.W., S.E.B., Z.Z., O.V.M.; software, S.E.B.; validation, G.R.W., S.B. and S.E.B.; formal analysis, S.E.B., Z.Z., O.V.M.; investigation, S.E.B., Z.Z., O.V.M.; resources, G.R.W.; data curation, S.E.B.; writing—original draft preparation, S.E.B.; writing—review and editing, S.E.B., G.R.W., S.B., Z.Z., O.V.M.; visualization, S.E.B.; supervision, G.R.W., S.B.; project administration, S.E.B.; funding acquisition, S.E.B., G.R.W. All authors have read and agreed to the published version of the manuscript.

Funding

We thank the Diamond Light Source for access to Beamline I12 under experiment MG28460-1, and TA Instruments Ltd. for donation of DSC equipment.

Declaration of Competing Interest

The authors declare that they have no known competing financial interests or personal relationships that could have appeared to influence the work reported in this paper.

Data availability

Data will be made available on request.

Acknowledgments

We thank Dr Kreso Bucar for access to the ball mill used in these experiments.

Appendix A. Supplementary data

Supplementary data to this article can be found online at <https://doi.org/10.1016/j.ijpharm.2023.123291>.

References

Amidon, G., Lennernäs, H., Shah, V., Crison, J., 1995. A theoretical basis for a biopharmaceutic drug classification: the correlation of in vitro drug product dissolution and in vivo bioavailability. *Pharm. Res.* 12, 413–420.

- Baghel, S., Cathcart, H., O'Reilly, N.J., 2016. Polymeric Amorphous Solid Dispersions: A Review of Amorphization, Crystallization, Stabilization, Solid-State Characterization, and Aqueous Solubilization of Biopharmaceutical Classification System Class II Drugs. *J. Pharm. Sci.* 105 (9), 2527–2544.
- Bakhtiari, S.E., Joubert, F., Pasparakis, G., Brocchini, S., Williams, G.R., 2023. Nanoparticle forming polyelectrolyte complexes derived from well-defined block copolymers. *Eur. Polym. J.* 189, 111977.
- Basham, M., Filik, J., Wharmby, M.T., Chang, P.C.Y., El Kassaby, B., Gerring, M., Aishima, J., Levik, K., Pulford, B.C.A., Sikharulidze, I., Sneddon, D., Webber, M., Dhesi, S.S., Maccherozzi, F., Svensson, O., Brockhauser, S., Náray, G., Ashton, A.W., 2015. Data Analysis Workbench (DAWN). *J. Synchrotron Radiat.* 22 (3), 853–858.
- Bergström, C., Luthman, K., P., A., 2004. Accuracy of calculated pH-dependent aqueous drug solubility. *Eur J Pharm Sci* 22, 387–398.
- Bhujbal, S.V., Mitra, B., Jain, U., Gong, Y., Agrawal, A., Karki, S., Taylor, L.S., Kumar, S., (Tony) Zhou, Q.I., 2021. Pharmaceutical amorphous solid dispersion: A review of manufacturing strategies. *Acta Pharm. Sin.* B 11 (8), 2505–2536.
- Clout, A., Buanz, A.B.M., Prior, T.J., Reinhard, C., Wu, Y., O'Hare, D., Williams, G.R., Gaisford, S., 2016. Simultaneous Differential Scanning Calorimetry-Synchrotron X-ray Powder Diffraction: A Powerful Technique for Physical Form Characterization in Pharmaceutical Materials. *Anal. Chem.* 88 (20), 10111–10117.
- Craig, D.Q.M., 2002. The mechanisms of drug release from solid dispersions in water-soluble polymers. *International Journal of Pharmaceutics* 231 (2), 131–144.
- Drakopoulos, M., Connolly, T., Reinhard, C., Atwood, R., Magdysyuk, O., Vo, N., Hart, M., Connor, L., Humphreys, B., Howell, G., Davies, S., Hill, T., Wilkin, G., Pedersen, U., Foster, A., De Maio, N., Basham, M., Yuan, F., Wanelik, K., 2015. I12: the Joint Engineering, Environment and Processing (JEEP) beamline at Diamond Light Source. *J. Synchrotron Radiat.* 22 (3), 828–838.
- Fan, W., Zhu, W., Zhang, X., Xu, Y., Di, L., 2019. Application of the combination of ball-milling and hot-melt extrusion in the development of an amorphous solid dispersion of a poorly water-soluble drug with high melting point. *RSC Adv.* 9 (39), 22263–22273.
- Filik, J., Ashton, A., Chang, P., Chater, P., Day, S., Drakopoulos, M., Gerring, M., Hart, M., Magdysyuk, O., Michalik, S., Smith, A., Tang, C., Terrill, N., Wharmby, M., Wilhelm, H., 2017. Processing two-dimensional X-ray diffraction and small-angle scattering data in DAWN 2. *J. Appl. Cryst.* 50, 959–966.
- Graessler, K.A., Patterson, J.E., Zeitler, J.A., Rades, T., 2010. The Role of Configurational Entropy in Amorphous Systems. *Pharmaceutics* 2, 224–244.
- Hart, M.L., Drakopoulos, M., Reinhard, C., Connolly, T., 2013. Complete elliptical ring geometry provides energy and instrument calibration for synchrotron-based two-dimensional X-ray diffraction. *J. Appl. Cryst.* 46 (5), 1249–1260.
- Hughes, D.L., 2017. Patent Review of Manufacturing Routes to Recently Approved PARP Inhibitors: Olaparib, Rucaparib, and Niraparib. *Org. Process Res. Dev.* 21 (9), 1227–1244.
- Khougaz, K., Clas, S.D., 2000. Crystallization Inhibition in Solid Dispersions of MK-0591 and Poly(vinylpyrrolidone) Polymers. *J. Pharm. Sci.* 89, 1325–1334.
- Konno, H., Handa, T., Alonzo, D.E., Taylor, L.S., 2008. Effect of polymer type on the dissolution profile of amorphous solid dispersions containing felodipine. *Eur. J. Pharm. Biopharm.* 70 (2), 493–499.
- Ku, M.S., 2008. Use of the Biopharmaceutical Classification System in early drug development. *AAPS J.* 10 (1), 208–212.
- Li, S., Doyle, P., Metz, S., Royce, A.E., Serajuddin, A.T.M., 2005. Effect of chloride ion on dissolution of different salt forms of haloperidol, a model basic drug. *J. Pharm. Sci.* 94 (10), 2224–2231.
- Lin, X., Hu, Y., Liu, L., Su, L., Li, N., Yu, J., Tang, B., Yang, Z., 2018. Physical Stability of Amorphous Solid Dispersions: a Physicochemical Perspective with Thermodynamic, Kinetic and Environmental Aspects. *Pharm. Res.* 35, 1–18.
- Liu, X.u., Ma, X., Kun, E., Guo, X., Yu, Z., Zhang, F., 2018. Influence of lidocaine forms (salt vs. freebase) on properties of drug-eudragit® L100–55 extrudates prepared by reactive melt extrusion. *Int. J. Pharm.* 547 (1–2), 291–302.
- Liu, H., Wang, P., Zhang, X., Shen, F., Gogos, C.G., 2010. Effects of extrusion process parameters on the dissolution behavior of indomethacin in Eudragit E PO solid dispersions. *Int. J. Pharm.* 383 (1–2), 161–169.
- Mesallati, H., Umerska, A., Paluch, K.J., Tajber, L., 2017. Amorphous Polymeric Drug Salts as Ionic Solid Dispersion Forms of Ciprofloxacin. *Mol. Pharm.* 14 (7), 2209–2223.
- Qin, Y., Xiao, C., Li, X., Huang, J., Si, L., Sun, M., 2022. Enteric Polymer-Based Amorphous Solid Dispersions Enhance Oral Absorption of the Weakly Basic Drug Nintedanib via Stabilization of Supersaturation. *Pharmaceutics* 14, 1–20.
- Serajuddin, A.T.M., 2007. Salt formation to improve drug solubility. *Adv. Drug Deliv. Rev.* 59 (7), 603–616.
- Šišak Jung, D., Donath, T., Magdysyuk, O., Bednarcik, J., 2017. High-energy X-ray applications: current status and new opportunities. *Powder Diffr.* 32, S22–S27.
- Sóti, P.L., Bocz, K., Pataki, H., Eke, Z., Farkas, A., Verreck, G., Kiss, É., Fekete, P., Vigh, T., Wagner, I., Nagy, Z.K., Marosi, G., 2015. Comparison of spray drying, electroblowing and electrospinning for preparation of Eudragit E and itraconazole solid dispersions. *Int. J. Pharm.* 494 (1), 23–30.
- Turner, D.T., Schwartz, A., 1985. The glass transition temperature of poly(N-vinyl pyrrolidone) by differential scanning calorimetry. *Polymer* 26 (5), 757–762.
- Warren, D.B., Benameur, H., Porter, C.J.H., Pouton, C.W., 2010. Using polymeric precipitation inhibitors to improve the absorption of poorly water-soluble drugs: A mechanistic basis for utility. *J. Drug Target.* 18 (10), 704–731.
- Xie, T., Taylor, L.S., 2016. Improved Release of Celecoxib from High Drug Loading Amorphous Solid Dispersions Formulated with Polyacrylic Acid and Cellulose Derivatives. *Mol. Pharm.* 13 (3), 873–884.
- Zotova, J., Wojnarowska, Z., Twamley, B., Paluch, M., Tajber, L., 2020. Green Synthesis of Lidocaine Ionic Liquids and Salts: Mechanisms of Formation and Interactions in

the Crystalline and Supercooled States. ACS Sustain. Chem. Eng. 8 (49), 18266–18276.